

INFLUENCE OF SURFACE TEXTURE ON DRAG REDUCTION OF SUPERHYDROPHOBIC SURFACES

C. T. Fairhall, R. Garcia-Mayoral

Department of Engineering, University of Cambridge, CB2 1PZ, Cambridge, UK

INTRODUCTION

Superhydrophobicity is caused by a surface roughness that can entrap pockets of gas between the roughness elements. For submerged surfaces, the liquid flowing above only ‘sees’ the no-slip surface at the roughness crests, with nearly free-shear over the gas pockets, as shown schematically in Figure 1. As the liquid is free to slip over the gas pockets, this greatly increases the slip length of the surface, which in turn can lead to a reduction in skin friction drag. This drag reduction behaviour has been observed both experimentally and numerically for laminar and turbulent flows [9]. The present work focuses on the slip effect of superhydrophobic surfaces. While much research has been conducted investigating flows with alternating no-slip/free-slip boundary conditions [8, 4, 3, 11], no clear arrangement to maximise the achievable slip length has yet been proposed.

Under turbulent conditions, and so long as the texture size is small, drag reduction effects for superhydrophobic surfaces are essentially limited to modifications of the flow within the viscous sublayer. The logarithmic layer is shifted away from the wall, but remains otherwise unmodified [2]. Under these conditions, the effect of superhydrophobic surfaces can be studied by considering the flow within the viscous sublayer only. In this region, the advective terms are negligible compared to the the viscous terms, and the governing equations can be simplified to the Stokes equations [5, 4], greatly decreasing the computational cost.

The work here provides an initial analysis to determine how the slip length of the surface varies with the surface pattern and gas fraction, in the limit of vanishing spacing. Several surface post arrangements have been investigated to determine which maximise the slip length. Further to this, the influence of the surface pattern on the deformation of the gas pocket has been considered as this is thought to be a key factor in the loss of the drag reduction effect [10].

NUMERICAL MODEL

For a vanishingly small surface texture, the pattern size is small compared to the turbulent structures in the above flow. The surface texture therefore does not see a variation in the flow conditions across many unit spacings. This allows the flow above the surface to be modelled as responding to an applied uniform shear (S). Since the surface pattern is periodic in both the streamwise and spanwise directions, a periodic simulation domain including a single pattern unit can be considered.

The model here assumes that the surface is flat, with no meniscus of the gas pocket, and does not deform. These simplifications are suitable for the case of vanishing spacing, and

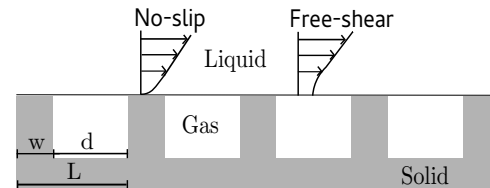


Figure 1: Schematic of a superhydrophobic surface showing the regions of no-slip and free-shear. w is the roughness width, d is the roughness spacing and L is the total size of the texture pattern.

imply that the surface can be modelled as a series of discrete free-shear/no-slip boundary conditions, as is often done in the literature [6, 7].

The parameters investigated in this study are the texture shape (ridges and posts), the influence of the gas fraction, post shapes, and the surface arrangement.

To calculate the slip lengths a fractional step method has been used, with an implicit time advancement scheme. The domain height is $2.5L$ in the wall-normal direction, where L is the texture spacing. A staggered grid has been used with $256 \times 64 \times 256$ grid points, stretched in the wall-normal direction, to give $\Delta x/L = \Delta z/L \simeq 0.004$, and $\Delta y_{min}/L \simeq 0.003$ at the surface.

RESULTS

The first set of results presented here show how the slip length is modified for different surface textures. The deformation of the gas pockets for these textures is then considered.

Figure 2 shows the influence of the gas fraction on the slip length for square, diamond and circular posts in a collocated arrangement, and for streamwise ridges. This figure shows that posts perform better at higher gas fractions than ridges, and vice versa for lower gas fractions, which is in agreement with [11]. The post shape has a minimal influence in the achieved slip length, with square and diamond posts having the same slip lengths, and with circular posts having only slightly higher slips. This is not however surprising, considering the flow is purely viscous. In this limit the drag of a free flow on an object does not depend on the objects orientation [1]. Though not shown here, we observe that that the post arrangement does not influence the slip length.

These results show that the particular texture arrangement, beyond the choice of ridges or posts, has only a small influence on the slip length. The arrangement can however have a significant impact on other important factors, such as the deformability of the gas pockets, which can eventually lead to their depletion. For post textures, the flow accelerates

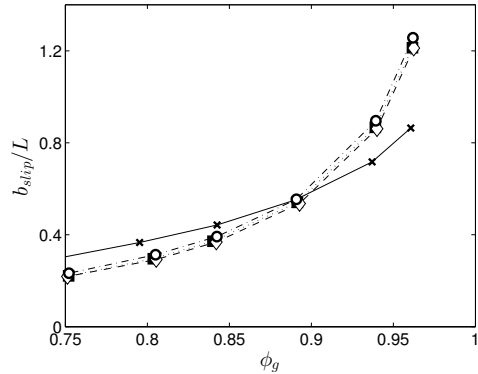


Figure 2: Influence of gas fraction on slip length for streamwise ridges ($-x-$), square posts ($\cdots \blacksquare \cdots$), diamond posts ($-- \diamond --$) and circular posts ($- \circ -$) for a collocated arrangement.

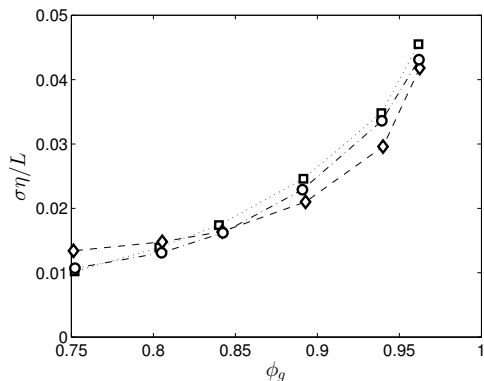


Figure 3: Influence of gas fraction on maximum gas pocket displacement for square posts ($\cdots \square \cdots$), diamond posts ($-- \diamond --$) and circular posts ($- \circ -$) for a collocated arrangement.

and decelerates between posts, causing a non-uniform pressure distribution over the gas layer [10]. While the model here assumes that the gas/liquid interface remains flat, and ignores pressure fluctuations from the overlying flow, the resulting pressure distributions can be used to estimate the interface deformations for different textures. These distributions can therefore provide a measure for the sensitivity of each texture layout to pressure effects. This is achieved by solving a Young-Laplace equation for the pressure distribution at the interface, $\nabla^2 \eta \approx \frac{\Delta P}{\sigma}$, where η is the interface displacement, ΔP is the interface pressure difference and σ is the surface tension.

The resulting maximum gas pocket deformation, as a function of gas fraction, are shown in Figures 3 and 4 for the collocated and staggered arrangements respectively. The displacement depends on both the post shape and the surface pressure distribution. For the collocated arrangement at low gas fraction the post shape has the largest influence, as the pressure variation remains relatively small. The diamond post suffers the highest deformation due to having the largest distance between post edges. However, as the gas fraction is increased the pressure distribution plays a key role, so that the circular and square posts perform the worst. As very large gas fractions are approached, influence of the post shape on the deformation is greatly reduced. For the staggered arrangement, the maximum deformation is higher, due to adjacent streamwise posts being further apart, which allows higher gas pocket deformation.

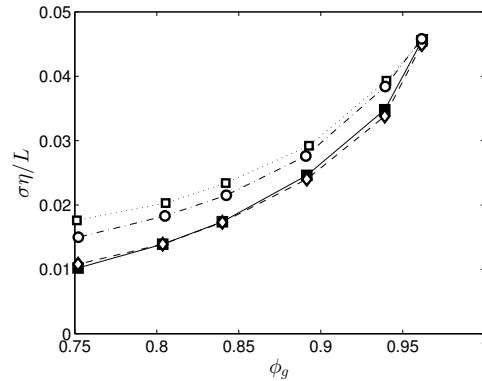


Figure 4: Influence of gas fraction on maximum gas pocket displacement for square posts ($\cdots \square \cdots$), diamond posts ($-- \diamond --$) and circular posts ($- \circ -$) for a staggered arrangement with the collocated square post arrangement ($- \blacksquare -$) for reference.

REFERENCES

- [1] G. K. Batchelor. *An Introduction to Fluid Dynamics*. Cambridge University Press, 14th edition, 2000.
- [2] F. H. Clauser. The turbulent boundary layer. *Adv. Appl. Mech.*, 4:1–51, 1956.
- [3] K. Fukagata, N. Kasagi, and P. Koumoutsakos. A theoretical prediction of friction drag reduction in turbulent flow by superhydrophobic surfaces. *Phys. Fluids*, 18:051703, 2006.
- [4] E. Lauga and H. A. Stone. Effective slip in pressure-driven stokes flow. *J. Fluid Mech.*, 489:55–77, 2003.
- [5] P. Luchini, F. Manzo, and A. Pozzi. Resistance of a grooved surface to parallel flow and cross-flow. *J. Fluid Mech.*, 228:87–109, 1991.
- [6] M. B. Martell, J. B. Perot, and J. P. Rothstein. Direct numerical simulations of turbulent flows over superhydrophobic surfaces. *J. Fluid Mech.*, 620:31–41, 2009.
- [7] H. Park, H. Park, and J. Kim. A numerical study of the effects of superhydrophobic surface on skin-friction drag in turbulent channel flow. *Phys. Fluids*, 25:110815, 2013.
- [8] J. R. Philip. Flows satisfying mixed no-slip and no-shear conditions. *Z. Angew. Math. Phys.*, 23:353–372, 1972.
- [9] J. P. Rothstein. Slip on superhydrophobic surfaces. *Annu. Rev. of Fluid Mech.*, 42:89–109, 2010.
- [10] J. Seo, R. Garcia-Mayoral, and A. Mani. Pressure fluctuations in turbulent flows over superhydrophobic surfaces. *Center for Turbulence Research - Annual Research Briefs 2013*, pages 217–229, 2013.
- [11] C. Ybert, C. Barentin, and C. Cottin-Bizonne. Achieving large slip with superhydrophobic surfaces: Scaling laws for generic geometries. *Phys. Fluids*, 19:123601, 2007.